Green Analytical Chemistry 17 (2026) 100332

Contents lists available at ScienceDirect

Green Analytical Chemistry

journal homepage: www.elsevier.com/locate/greeac

First-line electroanalytical screening platform for rapid detection of Alternaria toxins in fresh tomatoes based on chemically-modified screen-printed gold electrodes and Machine Learning predictive models

Simone Fortunati [a], Cristian Maffezzoni [a], Chiara Giliberti [a], Valentina Bianchi [b], Ilaria De Munari [b], Maria Careri [a], Marco Giannetto [a,*]

[a] Department of Chemistry, Life Sciences and Environmental Sustainability, University of Parma, Parco Area delle Scienze 17/A, 43124 Parma, Italy
[b] Department of Engineering and Architecture, University of Parma, Parco Area delle Scienze 181/A, 43124 Parma, Italy

ARTICLE INFO

Keywords:
Alternaria toxins
Tomato
Chemically Modified Electrode
Self-Assembled Monolayer
dodecanethiol
electrochemical detection
Machine Learning

ABSTRACT

The detection of Alternaria mycotoxins in food is a growing concern due to their potential health effects. Although HPLC-MS-based techniques are the most widely used for the accurate determination of mycotoxins, they are not suitable for rapid on-site screening, which emphasises the need for portable, cost-effective and environmentally friendly analytical instruments. In this study, we developed a first-line electroanalytical platform for the rapid detection of alternariol (AOH) and alternariol-9-methyl ether (AME) using screen-printed gold electrodes modified with dodecanethiol self-assembled monolayers (SAMs). Dodecanethiol SAM deposition was optimized using a 2^2 full factorial design to enhance and differentiate the electrochemical responses of each of the two toxins with even minimal structural differences, as confirmed by cyclic voltammetry and impedance spectroscopy. Good results with LOD and LOQ at the low μg/kg level were achieved, approaching the indicative levels recommended for the target compounds in processed tomato products. Very good inter-electrode repeatability with RSD <10% was also achieved. The integration of Machine Learning (ML) techniques into the analytical workflow was successfully evaluated to enable predictive modelling of contamination events using the dual-channel electroanalytical platform. The method requires minimal sample treatment, produces negligible waste, and is compatible with low-power portable devices. Finally, AGREE, ComplexMoGAPI and SPMS metrics were used to assess the greenness, proving excellent compliance with the principles of green analytical chemistry. For the first time we demonstrated the potential of the integration of ML into an environmentally friendly electrochemical platform to enable a cost-effective primary screening for these representative Alternaria toxins.

1. Introduction

Alternaria s.p. is a genus of Ascomycete fungi that includes several plant pathogens, responsible for a wide range of diseases in both agriculture and horticulture. Alternaria species produce secondary metabolites, or mycotoxins, that have emerged as a health concern because of their potential toxicity, being commonly found on grains, fruits, tomatoes and tomato-based products [1]. Alternaria toxins (ATs) can be classified into three distinct groups based on their chemical structure: dibenzopyrone derivatives (e.g., alternariol (AOH), alternariol monomethylether (AME), altenuene), perylene derivatives (e.g., altertoxin I, altertoxin II), and tetramic acid derivatives (e.g. tenuazonic acid (TeA)). These compounds are considered to be some of the important toxic metabolites of various *Alternaria* species occurring in food commodities [2].

Contamination by ATs, including AOH and AME, has been reported in a wide range of crops, notably tomatoes. The presence of AOH and AME in tomatoes can occur due to fungal contamination during growth, storage and transportation, and is often influenced by environmental and agronomic factors [3].

As consequence of these findings, the European Food Safety Authority (EFSA) issued opinions on ATs in 2011 and 2016, concluding that chronic dietary exposure to AOH, AME, and TeA exceeds levels of toxicological concern [4,5]. This is due to potential mutagenic, carcinogenic, and neurotoxic effects, which prompted requests for further toxicity data and a link to various health disorders, as demonstrated by

* Corresponding author.
E-mail address: marco.giannetto@unipr.it (M. Giannetto).

https://doi.org/10.1016/j.greeac.2026.100332
Received 19 December 2025; Received in revised form 29 January 2026; Accepted 1 March 2026
Available online 2 March 2026
2772-5774/© 2026 The Authors. Published by Elsevier B.V. This is an open access article under the CC BY license (http://creativecommons.org/licenses/by/4.0/).

epidemiological studies [6]. As a result, the presence of AOH and AME in tomatoes has prompted increased regulatory controls and the establishment of maximum residue limits (MRLs) for mycotoxins like AOH and AME, in food products, especially for tomatoes, but standardized monitoring guidelines are still lacking, highlighting the need for continued research and improved detection methods.

In such a context, the European Union has recently issued Recommendation (EU) 2022/553, inviting Member States to collect data on ATs in food using analytical methods suitable for monitoring at the indicative levels established for certain Alternaria toxins [7].

The detection and quantification of AOH and AME in fruits and tomatoes pose significant analytical challenges because they are present at low concentrations in complex matrices that include sugars, pigments, polyphenols and other organic compounds [8]. Overcoming this requires sensitive and selective analytical methods, often involving a multi-step process of extraction, purification using techniques like QuEChERS and molecularly imprinted polymer beads [9–11], and advanced analytical techniques, like liquid chromatography-tandem mass spectrometry (HPLC-MS/MS) or LC with high-resolution mass spectrometry [9,11–13] or gas chromatography-tandem mass spectrometry (GC-MS/MS) [14]. However, detection of Alternaria mycotoxins by GC implies a time-consuming and complicated derivatization to convert polar, non-volatile toxins into volatile forms, resulting in delays in analysis especially when large number of samples are to be analysed. Although the above-mentioned instrumental approaches boast numerous advantages, including high accuracy and sensitivity, they are expensive, require complex pretreatment and high level of expertise. However, these approaches fail to meet the needs for rapid and timely on-site screening; therefore, there is an urgent need to develop rapid, affordable, accurate, and sensitive screening methods for detecting Alternaria toxins to ensure the quality and safety of food products.

Among the available methodologies, enzyme-linked immunosorbent assays (ELISA) [15] and immunochromatographic strip tests as lateral flow immunoassays (LFIA) [16] offer promising approaches due to their simplicity, rapid detection, high specificity and good stability. ELISA allows for quantitative analysis but is generally not suitable for field analysis as it requires multiple steps and trained technicians, while LFIAs offer a naked-eye readout without the need for instrumentation providing qualitative or semi-quantitative information. Only very recently rapid immunoassays for on-site sensitive analysis of alternariol have been devised, but it should be noted that this work has focused on only one of the Alternaria mycotoxins [17]. In this scenario, the ideal solution as a compromise between sensitivity, rapid analysis, cost-effectiveness and smart portable instrumentation is represented by electrochemical sensors and biosensors. Among them, although aptasensors have recently been proposed as promising candidates for the effective detection of AOH [18–20], showing high sensitivity and wide detection range, the severe limitations of aptamers as receptors for sensing devices must be considered. These drawbacks have recently been demonstrated in terms of low robustness and strong dependence of their binding interactions on experimental factors such as ionic strength and electrolyte composition of the measuring medium [21,22].

Tyrosinase-based enzymatic biosensors have also been reported for the detection of Alternaria toxins. However, they have several disadvantages, including the high cost of the enzyme receptor, the need for rigorous pH and temperature control, and poor performance in the determination of AOH and AME toxins. These limitations also extend to their application in food analysis, where their effectiveness has not yet been fully explored [23].

In this scenario, the development of electroanalytical methods that avoids the use of biological receptors offers clear advantages in terms of low fabrication costs, analytical robustness, durability and lifetime. Among these, Chemically Modified Electrodes (CMEs) *via* Self-Assembled Monolayers (SAM) of heterobifunctional molecules represent analytical solutions with an excellent cost-performance balance [24–26].

SAMs have established themselves as powerful tools in the development of electroanalytical devices, offering unique advantages in terms of surface functionalization, stability, and sensitivity [24]. These monolayers consist of molecules that spontaneously organize into a well-ordered layer on a substrate, typically gold or other metals, thanks to interactions between a bifunctional molecule and the sensing surface. In the context of electroanalytical devices, SAMs play a fundamental role in regulating electrode surface properties, including charge transfer, electrochemical stability, and the ability to mediate redox processes towards target analytes. Furthermore, SAMs offer the advantage of being cost-effective, easy to prepare and versatile, enabling the design of highly functional systems adaptable to different signal transduction principles.

In this context, in the present study a simple, rapid, eco-friendly and cost-effective electroanalytical platform based on two CMEs featuring screen-printed gold electrodes derivatized with dodecanethiol SAMs was developed and optimized for the detection of AOH and AME in fresh tomato samples using differential pulse voltammetry (DPV). These Alternaria toxins are chosen as representatives for this relevant compound class. The use of experimental design techniques for the optimization of the CMEs enabled the development of a dual-channel system allowing for sensitive and rapid detection of the two major Alternaria mycotoxins. Furthermore, as successfully demonstrated in our previous studies [27,28], the integration of Machine Learning (ML) techniques into the analytical workflow was evaluated to enable predictive modelling of contamination events. As recently reviewed, ML algorithms are increasingly combined with electroanalytical techniques to analyze complex signals and harness their potential for high specificity and sensitivity [29,30]. The implementation of ML classifiers to process electrochemical voltammetric signals enabled the rapid detection of non-compliant tomato samples at low levels of AOH and AME contamination by distinguishing them from compliant ones. This approach can be used to develop rapid and reliable food safety tools, potentially embedding them in portable devices for real-time analysis. Furthermore, thanks to the time- and cost-effectiveness of the entire analytical process and the ability to integrate with portable and low-power consuming readout instrumentation, the developed methodology fulfils most of the twelve principles of green analytical chemistry, obtaining excellent greenness ratings by applying AGREE [31], ComplexMoGAPI [32] and SPMS [33] as three different analytical greenness metric tools.

To our knowledge this is the first proof-of-concept study demonstrating the potential of the integration of ML into an environmentally friendly DPV electrochemical method for application in the food production sites to enable a cost-effective primary screening for these Alternaria toxins.

2. Materials and methods

2.1. Chemicals and materials

1-Dodecanethiol (DDT), acetone, ethanol 96%, acetonitrile, alternariol from *Alternaria sp* (AOH), alternariol-9-methyl ether from *Alternaria alternata (tenuis)* (AME), disodium hydrogen phosphate (Na_2HPO_4), sodium dihydrogen phosphate (NaH_2PO_4), potassium dihydrogen phosphate (KH_2PO_4), potassium ferrocyanide ($K_4[Fe(CN)_6]$) were purchased from Sigma-Aldrich (Milan, Italy).

Fresh tomatoes of the *Fokker* variety, a cultivar typically used in industrial production, were purchased from a local store.

Screen-Printed Gold Electrode DRP-220 BT (SPGE) with 0.2 cm radius gold working electrode cured at low-temperature (around 150° C) and silver pseudoreference electrode were purchased from Metrohm Italiana SRL (Origgio, Varese, Italy).

Ultrapure water (18.2 MΩ·cm) was obtained from a Direct Q® 3 UV ultrapure water system.

Phosphate Buffered Saline (PBS) was prepared with the following composition: 137 mM NaCl, 2.7 mM KCl, 1.2 mM KH_2PO_4, and 8 mM

Na_2HPO_4 (pH= 7.4).

Composition of the reading buffer for AME and AOH measurements was: 40% 0.5 M NaH_2PO_4, 40% 0.4 M Na_2HPO_4 with an addition of 20% acetonitrile (pH=7.0).

2.2. Sample preparation

Fresh tomatoes were washed, cut and frozen in liquid nitrogen before being ground in a mill. The resulting homogenized material was then transferred to 50 mL Falcon tubes, thawed to +4°C and centrifuged for 10 minutes at 4000 rpm, maintaining the temperature at +4°C throughout. The supernatant was then collected and stored until analysis.

AOH and AME were dissolved in acetone and acetonitrile, respectively, to obtain 500 mg/L standard solutions. These solutions were then diluted to the appropriate concentrations in a 1:1 mixture of centrifuged tomato sample and reading buffer.

Starting from one sample of the Fokker cultivar, a total of 45 centrifuged tomato samples were prepared and analyzed, including control samples (n=15), samples spiked with 0.5 mg/L AOH (n=15) and with 0.5 mg/L AME (n=15). Before spiking, the absence of AOH and AME contamination in centrifuged tomato samples was assessed by QuEChERS method coupled with UHPLC-MS/MS [34].

2.3. Equipment

Electrochemical measurements were performed using a Multi Autolab M204 10-channel potentiostat/galvanostat (Metrohm Italiana Srl, Origgio, Varese, Italy), equipped with the FRA32M electrochemical impedance spectroscopy (EIS) module. The instrument was controlled *via* NOVA 2.1.6 Advanced Electrochemical Software. The SPEs were connected to a boxed connector from DropSens (Origgio, Varese, Italy; DRP-DSC), which allowed them to be interfaced with the potentiostat.

A pHmeter Violab pH 60/XS (XS Instruments, Carpi, Modena, Italy) was used for pH measurements. SPGEs were modified using a heating magnetic stirrer AREX from VELP Scientifica (Biosigma, Cona, Venice, Italy).

IKA a11 basic analytical mill (IKA-Werke GmbH & Co.KG, Staufen, Germany) and Eppendorf Centrifuge 5810R (Eppendorf, Hamburg, Germany) were used for sample treatment.

2.4. Electrode modification and electrochemical measurements

Two sets of electrodes were modified with a self-assembled monolayer by depositing DDT on the SPGE surface under optimized conditions. Specifically, the CMEs were prepared by dipping the electrodes in 5 mL of stirred ethanol solutions of DDT, using concentrations and deposition times that had been optimised for AME and AOH detection, respectively.

Electrochemical measurements were performed using DPV by scanning the potential from 0 V to +1 V with a step potential of 0.01 V, a modulation amplitude of 0.05 V, a modulation time of 0.1 s and an interval time of 0.5 s.

2.5. Experimental Design and Statistical Analysis

A two-level two-factor (2^2) full factorial design (FFD) was used to analyse factors involved in the fabrication of CMEs and find the optimal conditions for chemically modifying SPEs using DDT to individually detect AME and AOH. DDT concentration and deposition time were investigated as experimental factors. Two coded levels (- 1, +1) were used as follows: *DDT concentration* = 5 (-1), 20 (+1) mM; *deposition time* = 5 (-1), 15 (+1) min. The optimized response variable was the signal-to-noise (S/N) ratio obtained by analysing tomato samples spiked with 0.1 mg/mL AOH or AME and control tomato samples. Each experiment was performed in duplicate and in randomized order to minimize systematic bias.

A two-way Analysis of Variance (ANOVA) with Bonferroni post-hoc test was carried out to assess the significance of the two factors and their interactions. The resulting dataset was analysed through multiple linear regression (MLR) to obtain the response function and assess the optimal experimental conditions for the detection of AOH and AME, respectively.

Statistical analysis was carried out using the Statistics for Data Analysis V.28 software package (SPS Srl, Bologna, Italy).

2.6. Electrochemical characterization of CMEs

The characterization of CMEs obtained by functionalization of SPGEs with SAMs of DDT was carried out using Cyclic Voltammetry (CV) and Electrochemical Impedance Spectroscopy (EIS). In both cases, a potassium ferrocyanide solution with a concentration of 1 mM in PBS was used as the redox probe. CV was performed by scanning potential between -0.25 and +0.75 V for 3 scans with a scan rate of 0.1 V/s. As for EIS experiments, a 5-mV amplitude sine wave perturbation was applied to the electrode, and the voltage was set at 0.19 V *vs* Ag pseudoreference according to the half-wave potential exhibited by the redox couple. The frequency range explored extended from 0.25 Hz to 10 kHz. The impedance spectra were reported as Nyquist diagrams where $-Z'' = f(Z')$, the imaginary part of the impedance, usually as $-Z''$, is plotted versus the real part of impedance, Z', at each excitation frequency [35].

2.7. Analytical validation

The analytical validation of the CME-based method was performed according to EURACHEM Guidelines [36] using matrices containing no detectable AOH and AME as blank samples. Measurements were carried out using tomato samples diluted 1:1 in read buffer and spiked with AME and/or AOH at various concentrations. Each CME was used for a single DPV scan and disposed after use.

The limit of detection (LOD) and limit of quantification (LOQ) were calculated as $3 \cdot s_0/\sqrt{n}$ and $10 \cdot s_0/\sqrt{n}$, respectively, where s_0 is the standard deviation measured on 10 replicated blanks and n is the number of replicate measurements.

Working linear range was assessed by testing analyte concentrations in the 0.1 - 1 mg/L range for both AOH and AME by applying Mandel's fitting test. The significance of the intercept (significance level 5%) was established by running a Student's t -test. Regression residuals were calculated, and the mean was not significantly different from zero ($p > 0.05$) over the working linear range for each mycotoxin. Precision in terms of inter-CME repeatability was calculated by performing 3 replicated measurements for each concentration level. Recovery rates were assessed by performing 3 replicated measurements of tomato samples spiked with two concentration levels of each toxin.

2.8. ML algorithms for data processing

The experimental datasets used to train and validate the ML models were obtained from the DPV analysis of tomato samples. The dataset was structured as follows:

- 3 sample classes were considered, namely control tomato samples and tomato samples spiked with 0.5 mg/L of either AOH or AME.
- 15 samples for each class were tested with both CMEs, obtaining 90 voltammograms.
- 100 current and potential values were acquired during each DPV scan.
- 1 current value and its corresponding potential were extracted from each DPV scan.

To train and validate the models, data obtained from the analysis of each individual sample performed with both CMEs were used. For this

purpose, datasets were constructed using either full DPV scans or specific sets of peak current and potential values (see Section 3.5).

Both datasets were randomly partitioned into cross-validation and testing subsets, with 80% of the data assigned to training and validation and the remaining 20% for testing. To ensure class balance, this partitioning was performed separately for each class. Furthermore, to enhance the reliability of the performance estimates, a 5-fold cross-validation procedure was applied to the training/validation subset.

The selection of data preprocessing criteria was driven by two primary rationales based on the dataset in use. Pareto scaling [37], a data handling technique that has been shown to reduce the influence of higher values while preserving part of the original structure of the dataset, was applied to the entire DPV dataset, while autoscaling was used for the dataset based on the extraction of peak current and potential values.

Unsupervised Principal Component Analysis (PCA) was carried out to exploratory evaluate each dataset and recognise features that enable differentiation between the three sample classes.

Data processing was performed using the Python programming language (version 3.11.13) with the aid of the PyCaret package (version 3.3.2) to automate the search for the best classification models [38]. The models demonstrating optimal performance were then optimised and validated individually using scikit-learn package (version 1.4.2) [39].

A total of ten ML algorithms were applied and compared in terms of their classification performance for different sample classes. Linear Discriminant Analysis (LDA), Partial Least Squares Discriminant Analysis (PLS-DA), Decision Tree (DT) and non-parametric K-Nearest Neighbors (KNN), both Euclidean and cubic,were evaluated as supervised approaches. Linear Support Vector Machine (SVM) was also tested as supervised classifiers to identify the most effective decision boundary for separating classes. This is achieved by identifying the hyperplane that maximises the distance between samples and the decision boundary [40]. Random Forest (RF) and Extra Trees (ET) were investigated as ensemble ML algorithms based on sets of decision trees: unlike RF [41], ET introduces more randomness, thus reducing variance and the risk of overfitting. Its effectiveness has been particularly demonstrated when applied to noisy datasets characterized by high variance [42]. In addition, we assessed the performance of the Naive Bayes (NB) classifier as a probabilistic model characterised by extreme speed and low computational requirements [43]. Finally, the sequential ensemble Gradient Boosting Classifier (GBC) method was also implemented: unlike RF, which is based on independent trees, GBC generates trees sequentially, with each tree correcting the errors of the previous one. This approach has been demonstrated to improve accuracy, promote flexibility, and mitigate bias [44].

We applied each model to both cross-validation and test set, using metrics of accuracy, precision, recall and F1-score, which is the harmonic mean of precision and recall.

3. Results and discussion

3.1. Working principle of CMEs

The electrochemical behaviour of polyphenolic derivatives, the class to which AOH and AME belong, is a complex phenomenon involving EC-type mechanisms. In these processes, proton abstraction corresponds to the chemical reaction (C), followed by multiple one-electron charge-transfer electrode steps (E). The phenoxonium ions involved can undergo further chemical reactions, namely the generation of dimers or polymers, thus inducing fouling phenomena on the surface of the bare gold electrode due to the accumulation of oxidation products. A further significant drawback is the oxidation potentials close to the onset of gold oxide formation [45]. These limitations can be overcome by using DDT-coated gold electrodes, since SAM plays an antifouling role, thus hindering the formation of gold oxides and surface passivation by electrochemical oxidation products without affecting the oxidation kinetics of AME [46]. This study demonstrates for the first time that the CME response to AOH or AME can be preferentially modulated through experimental optimisation of the DDT SAM deposition conditions. Although the small structural difference between AOH and AME does not allow voltammetric discrimination in terms of oxidation potential, the presence of the methoxide group in AME results in a slight difference in the relationship between structure and electrochemical properties, which translates into appreciable differences in the previously discussed EC mechanisms mediated by the DDT-based SAM.

3.2. Optimization of AOH/AME measurement

A 2^2 FFD was performed to optimise the chemical modification of SPGE with SAMs of DDT by studying the effects of two main factors on the electrochemical responses of AOH and AME. Two-way ANOVA with Bonferroni post-hoc test confirmed the significance of the effects of DDT concentration and deposition time, as well as their interaction ($p < 0.01$), for both mycotoxins investigated, as illustrated in the interaction plots shown in Fig. 1. In particular, Fig. 1a illustrates the signal-to-noise (S/N) ratio, obtained by analysing tomato samples spiked with 0.1 mg/mL AOH compared to blank tomato samples. Confidence intervals calculated using Fisher's Least Significant Difference (LSD) method are plotted as a function of DDT concentration for the two different deposition times. Similarly, Fig. 1b shows the electrochemical responses of AME under the same experimental conditions.

ANOVA interaction plots show that main effects and interactions exist. This means each factor independently accounts for variability in the dependent variable, but also, they appear to interact synergistically to explain the variance in the dependent variable. They combine uniquely to influence the AOH or AME response, where the best outcome for AOH in terms of high response occurs at specific combined levels (high DDT concentration, short deposition time) and different combinations (low DDT concentration, long deposition time) favor the AME response.

Based on these findings, the dataset was processed using multiple linear regression (MLR) to assess the optimal DDT deposition conditions for the detection of AOH and AME, respectively. The response functions calculated by MLR are reported in equations (1) and (2), where CME_{AOH} and CME_{AME} are intended as chemically modified electrodes optimized for the detection of AOH and AME, respectively, t is the deposition time (min) and $[DDT]$ is the dodecanethiol concentration (nM) used for the deposition of the SAMs; the standard deviations for each coefficient are reported in parentheses.

$$\boldsymbol{CME_{AOH}}: S/N = -1,133(0,136) + 0,041(0,004)\cdot t + 0,399(0,052)\cdot[DDT] - 0,018(0,002)\cdot t\cdot[DDT] \quad (1)$$

$$\boldsymbol{CME_{AME}}: S/N = -1,762(0,194) + 0,473(0,062)\cdot t + 0,067(0,006)\cdot[DDT] - 0,016(0,001)\cdot t\cdot[DDT] \quad (2)$$

The optimized t and $[DDT]$ values were as follows: 5 min and 20 mM for CME_{AOH}, 15 min and 5mM for CME_{AME}.

The optimized CME_{AOH} and CME_{AME} were tested for DPV responses of tomato centrifuged samples spiked with 0.5 mg/mL of AOH or AME, or with a mixture of AOH and AME each at a concentration of 0.25 mg/mL, as well as blank tomato centrifuged samples. As shown in Fig. 2, the results of these experiments indicate that, although the two CMEs are not intrinsically selective, they allow for enhanced detection of one toxin or the other when optimised for AOH or AME response. Good inter-CME repeatability with RSD below 10% (n=3) was obtained with both CMEs, as shown in Fig. S1.

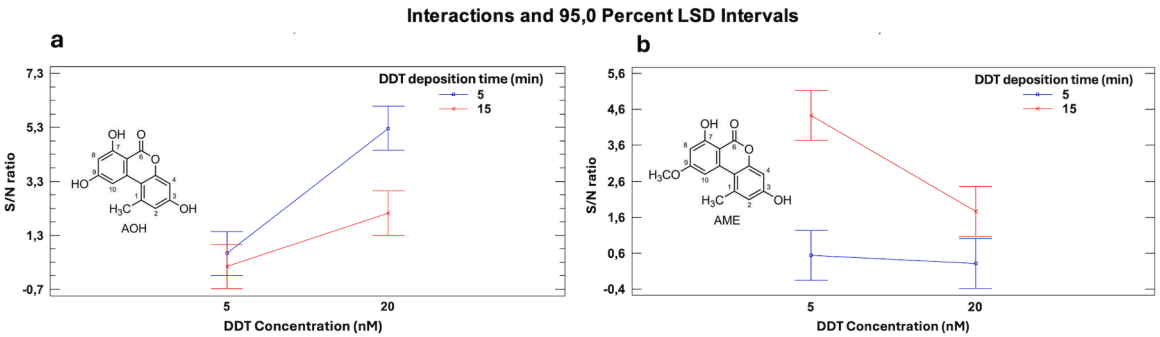


Fig. 1. ANOVA interaction plot and 95 percent LSD intervals as a function of DDT concentration considering two deposition times with reference to AOH (a) and AME (b).

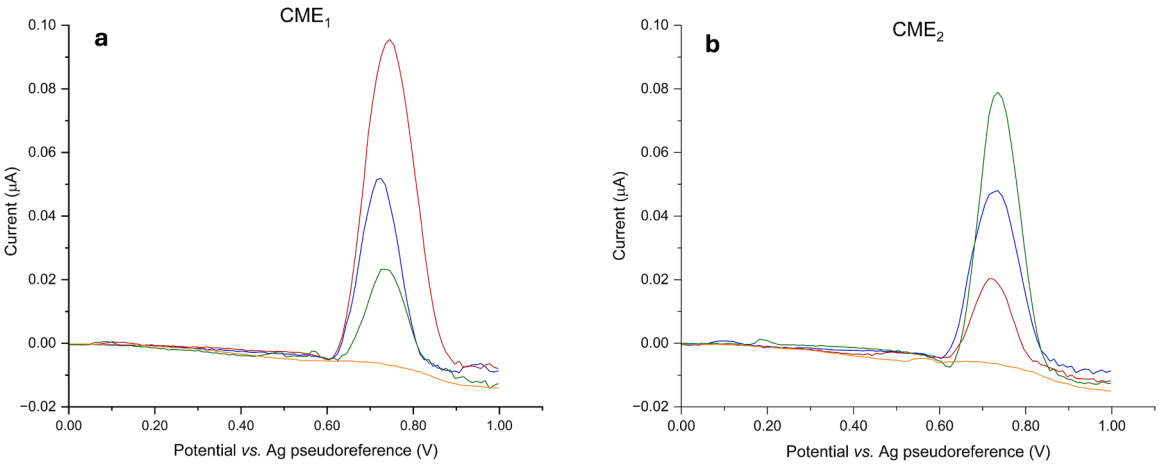


Fig. 2. DPV of tomato samples spiked with 0.5 mg/L of AOH (red line), 0.5 mg/L of AME (green line), a mixture of AOH and AME each at a concentration of 0.25 mg/mL (blue line), and control tomato samples (orange line) on CME_1 (a) and CME_2 (b).

These findings are an interesting result from the perspective of a combined approach involving the integration of the two CMEs into a multichannel electroanalytical platform aimed at a rapid, simple and cost-effective first screening for Alternaria-related mycotoxins in fresh tomato samples.

3.3. *Characterization of CME_s by CV and EIS*

Based on the different AOH and AME responses on the optimized CMEs in terms of DDT SAM deposition conditions, each modified electrode was characterized both by CV and EIS with the aim of investigating the influence of deposition conditions on SAM properties and then electrode/solution interfacial properties of the two SAMs. For both

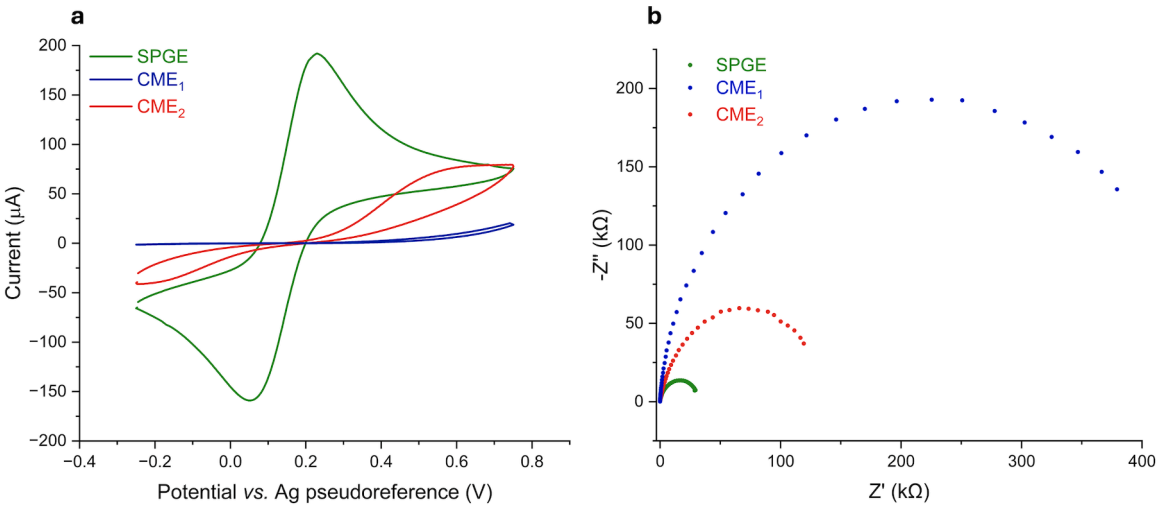


Fig. 3. Cyclic voltammograms (a) and Nyquist plots observed for electrochemical impedance spectra (b) on bare SPGE, CME_1 and CME_2 using 1 mM potassium ferrocyanide in PBS as redox probe.

characterization techniques, 1 mM potassium ferrocyanide in PBS was used as a redox probe. The results of the voltammetric characterization are illustrated in Fig. 3a, which shows how, in the case of $CME_{AOH,}$ SAM deposition in the optimized conditions resulted in a drastic decrease in the diffusion current of the redox probe compared to the standard response in the cyclic voltammogram of SPGE with unmodified gold electrode surface. A similar, though less pronounced, effect was observed in the case of CME_{AME} using a lower DDT concentration and longer deposition times.

Consistently, the impedimetric characterization of the two coatings via EIS confirmed the trend observed by CV (Fig. 3b). In fact, Nyquist plots showed a low charge transfer resistance (R_{ct}) for bare SPGE, with values lower than 50 kΩ, while the R_{ct} value increased to over 100 kΩ for CME_{AME} and further increased to over 400 kΩ for CME_{AOH}.

The overall evaluation of voltammetric and impedimetric data provides an explanation for the different AOH and AME responses on CMEs optimized for the two toxins. Although SAM deposition results in voltammetric responses with low current values due to the high charge transfer resistance of these sensing coatings, they play a fundamental role in terms of antifouling properties. This allows for the mediation of electron transfer processes, which is crucial for the detection of compounds with complex electroactivity, such as polyphenols. Therefore, by optimising SAM deposition conditions, it is possible to modulate these electron transfer mediation processes, thus inducing improved responses for each of the two toxins belonging to the same class but with even minimal structural differences.

3.4. Analytical performance of CME_s for the measurement of AOH and AME in tomato samples

The electrochemical method based on the use of CMEs was validated using 1:1 diluted tomato centrifuged samples spiked with AOH or AME at concentrations ranging from 0.1 to 1 mg/L.

Good results with LOD and LOQ values at the low μg/kg level were achieved for the target compounds, only slightly above the indicative level established for alternariol and alternariol monomethyl ether in processed tomato products, thus demonstrating the capabilities of DPV on the optimized CMEs for the detection and measurement of the most representative ATs in tomatoes at trace levels, taking into account that the indicative levels are not food safety levels [7]. The validation parameters of both CMEs are shown in Table 1.

Good linearity was also demonstrated by applying Mandel's fitting test across the explored working range for AOH using CME_{AOH} and AME using CME_{AME}: the mean of the calculated regression residuals was found to be not significantly different from zero *($p>0.05$)*.

Very good inter-electrode repeatability was observed for both CMEs, with RSD levels below 10% (n=3) for all levels of the calibration curves established for AOH and AME, ensuring the reliability and validity of electrochemical measurements considering the application of the developed platform to food safety assessment. To ensure that the signal was not lost during sample preparation and to evaluate any measurement bias, the recovery rate for both toxins was evaluated. Good recovery values were calculated: 99 ± 3% at 0.3 mg/L and 108 ± 6% at 0.9 mg/L for the detection of AOH, and 103 ± 7% at 0.3 mg/L and 97 ± 6% at 0.9 mg/L for the detection of AME.

Table 1
Validation parameters of the electrochemical method based on CME_{AOH} and CME_{AME}.

Toxin	b_1 (± s_{b1})[a,b]	LOD (mg/L)	LOQ
AOH	0.213 (± 0.006)	0.018	0.05
AME	0.067 (± 0.004)	0.027	0.09

[a] Regression equation: $y = b_0 + b_1 \cdot x$; $n=15$
[b] b_0 not significant *($p>0.05$)*

Although the developed electroanalytical platform does not rely on specific bioreceptors and thus cannot guarantee voltammetric discrimination between AOH and AME, it was found to be effective in determining the prevalence of each of the two toxins. It is important to emphasise that the use of bioreceptors, such as enzymes, makes the sensors expensive and does not intrinsically improve analytical performance compared to voltammetric determinations not mediated by bioreceptors. For instance, as reported by other authors, the modification of glassy carbon electrodes with the enzyme tyrosinase for the determination of AOH and AME produced significantly worse results than the electroanalytical platform proposed here, with detection limits in the order of 5 mg/L [23]. Furthermore, this approach has not been tested in any real matrix nor on food samples.

Regarding methods based on antibody receptors, even the most sensitive immunochemical methods with spectrophotometric reading (e.g. ELISA) do not provide any discrimination between AOH and AME. Even though these methods reach detection limits in the ng/mL range, they only allow a total assessment of the concentration of both toxins combined [15–17].

Although the working principle of dodecanethiol-based SAM for voltammetric detection of AME, based on its antifouling properties, has been previously investigated, validation of the electrochemical method for the quantitative determination of AME has been performed in terms of detection limit and response linearity only in buffer solutions [25]. Conversely, in this work voltammetric determination of Alternaria toxins mediated by a DDT SAM in a food matrix was successfully applied for the first time to tomato matrices, despite their high polyphenol content.

This finding is highlighted by the DPV curves that show no peak-shaped signals indicating the absence of redox-active species in the control samples. Furthermore, this behaviour was confirmed by comparing the voltametric responses obtained for the tomato control samples with the DPV pattern obtained for the reading buffer used for sample dilution (see Fig. S2). The comparable voltametric profiles provide evidence for selectivity, showing that the electroactive compounds present at high concentration in the tomato matrix do not interfere with the voltametric detection of AOH and AME mediated by DDT SAMs, thus excluding the occurrence of false positives.

Given the speed of the measurement technique and the use of portable, low-cost instrumentation, together with the potential for further improvements in SAM fabrication using other electrodes and other materials to chemically modify the electrodes, this is the first proof-of-concept study demonstrating the capabilities of DPV on optimized CMEs as a cost-effective test system for application at production sites, enabling first-line screening of these emerging representative ATs in tomatoes at trace levels.

3.5. Sample classification models by machine learning algorithms

Taking into account that information-rich electrochemical data hold great potential for ML, detecting specific analytes in complex matrices is challenging due to signal interference from other target or non-target compounds. Key strategies to overcome these challenges involve advanced ML models for pattern recognition and developing methods to assure that electrochemical systems can produce representative datasets with reasonable variability across different targets, such as using different electrodes with different surface chemistries to generate distinct responses for each analyte.

The development of pattern recognition models is valuable for implementing a rapid, simple and high-throughput electroanalytical method in point-of-need (PON) settings. In this work, processing the DPV dataset using the ML algorithms described in Section 2.8 allowed us to train and validate sample classification models with the aim of discriminating between uncontaminated (control) tomato samples and those spiked with AOH or AME at 0.5 mg/L each. ML models were applied to both the entire voltammetric dataset and the extracted peak

current and potential data, achieving better results in the latter case. We performed an automated peak search using the embedded feature in the NOVA 2.1.6 software to extract peak current and potential values from each DPV scan. Although this operation only takes few seconds, it is worth noting that it can become considerably labour-intensive for large datasets. In terms of energy consumption in data management, the peak search operation does not significantly impact the overall dataset acquisition and processing.

First, PCA was applied as an unsupervised technique with the purpose of data exploration and mining, showing that the intrinsic variance of the peak potential and current values of the three sample classes allows for good discrimination. The first two Components account for 79% of the variation in the data, with PC1 covering more than 59% of the total variance (see Figure S3a). These findings provided the basis for the successful implementation of ML classification models for more advanced predictive tasks, as we were also interested in analyzing whether voltammetric data could be used to predict AOH or AME contamination in tomato samples. The next step in the data processing methodology involves the use of supervised ML-based classification algorithms. As shown in Table 2, the best results were obtained using the NB, DT, RF and GBC classifiers, which provided remarkably high classification metrics, indicating high reliability with 1.00 accuracy in cross-validation and strong predictive power on unseen data (1.00 accuracy on the test set). As for the KNN algorithm, the classification model's performance is quite good, with 0.92 and 1.00 accuracy for cross-validation and test data, respectively. By contrast, the supervised algorithms PLS-DA, LDA and SVM performed less accurately or effectively compared to the other classifiers. In particular, PLS-DA performed the worst, likely because it struggled with complex patterns, or faced issues like overfitting or sensitivity to noise. Table 2 reports the accuracy, precision, recall and F1-score obtained with the different ML classifiers for both the cross-validation and test sets. An analysis of these metrics highlights the excellent performance of the classification models. In addition to accuracy, excellent values for precision, recall, and F1-score typically mean values close to 1.0, showing that the model's predictions align very closely with the actual outcomes Indeed, precision provides information on the extent to which each individual class is correctly classified, the recall score focuses on false negatives occurrence, while F1 score the harmonic mean balancing both accounting for both false positives and false negatives. The confusion matrices illustrated in Fig. 4 offer an insightful technique for visualizing the classifier performance of the four best-performing algorithms.

In a next step, with the aim of reducing the environmental impact, time and costs associated with the entire analytical process, we applied different ML algorithms to the entire DPV pattern without extracting peak current values. Indeed, avoiding peak search saves time during dataset preprocessing for the train and validation of prediction models and, more importantly, for the classification of unknown samples based on these ML models.

To handle noisy data such as entire DPV curves, Pareto scaling was used as a pre-processing strategy focusing on crucial features (peak height/position) while preserving their relative importance for the analysis [37]. Furthermore, as expected, given the intrinsic noise in the DPV dataset, exploratory PCA processing did not provide satisfactory results (Fig. S3b). Nevertheless, applying two ML algorithms allowed us to achieve excellent classification performance even with this data. In particular, the Naive Bayes approach, previously successfully applied to the reduced dataset, provided excellent classification metrics. This probabilistic model is indeed known for its ability to handle high-dimensional data [43]. The Extra-trees algorithm also provided excellent performance for the test set and even better results for cross-validation. The classification metrics for all ML models applied to the entire DPV dataset are shown in Table S1, while the corresponding confusion matrices for the best-performing models are shown in Figure S4. It is worth noting that the NB model performs successfully on both types of datasets, allowing for excellent sample classification without the need for peak current and potential extraction from the DPV dataset.

3.6. Greenness assessment of the electroanalytical screening platform

A further objective of this study is to develop an environmentally friendly DPV method for screening target ATs. The environmental impact of the proposed electroanalytical platform was assessed using three analytical greenness metric tools. Specifically, AGREE [31] and Complex Modified Green Analytical Procedure Index (ComplexMoGAPI) [32] were used to assess the overall environmental footprint of the proposed method, taking into account the entire analytical procedure from sampling to sample treatment and final measurement. These metric tools consider all 12 principles of Green Analytical Chemistry to assess sustainability and emphasizes environmental impact [47,48]. In addition, SPMS [33] was applied as metric tool aimed specifically at evaluating the impact of the sample treatment process, even if the analytical method here proposed does not involve laborious extraction and cleanup steps, but only grinding, centrifugation and dilution of the sample.

The overall results obtained for each metric tool are shown in Fig. 5, while the scores achieved for each specific criterion of the AGREE and ComplexMoGAPI metrics are summarized in Table 3. As for AGREE, considering that the metric operates according to the principle of assigning a total score of 100 points for an ideal green analysis, the proposed method showed a score of 0.77, with a predominantly green hue (Fig. 4a). It is noteworthy that we applied equal weight to each of the 12 indicators in calculating the score which, when it reaches a value greater than 0.75, indicates an excellent level of eco-sustainability and a highly environmentally friendly procedure.

The ComplexMoGAPI tool consistently returned an overall score of 78, classifying the proposed electroanalytical screening platform as an excellent green analytical approach ($\geq$75), according to a scoring scale that classifies methods as inadequately green if the score is less than 50 and as acceptable green if the score is in the range 50-74. The overall score assessment is shown in Fig. 4b, and the colour of the scale around

Table 2
Classification metrics for ML algorithms applied to the dataset derived from DPV (specifically peak currents and potentials). The results of the best classifiers are highlighted in bold.

Model	Cross-validation				Test set			
	Accuracy	Precision	Recall	F1-score	Accuracy	Precision	Recall	F1-score
PLS-DA	0.28	0.10	0.30	0.16	0.44	0.15	0.33	0.21
SVM	0.78	0.87	0.77	0.78	0.89	0.89	0.89	0.87
LDA	0.83	0.89	0.83	0.84	0.89	0.89	0.89	0.87
KNN-cubic	0.86	0.91	0.86	0.87	1.00	1.00	1.00	1.00
KNN-Euclidean	0.92	0.93	0.91	0.92	1.00	1.00	1.00	1.00
NB	1.00	1.00	1.00	1.00	1.00	1.00	1.00	1.00
DT	1.00	1.00	1.00	1.00	1.00	1.00	1.00	1.00
RF	1.00	1.00	1.00	1.00	1.00	1.00	1.00	1.00
GBC	1.00	1.00	1.00	1.00	1.00	1.00	1.00	1.00

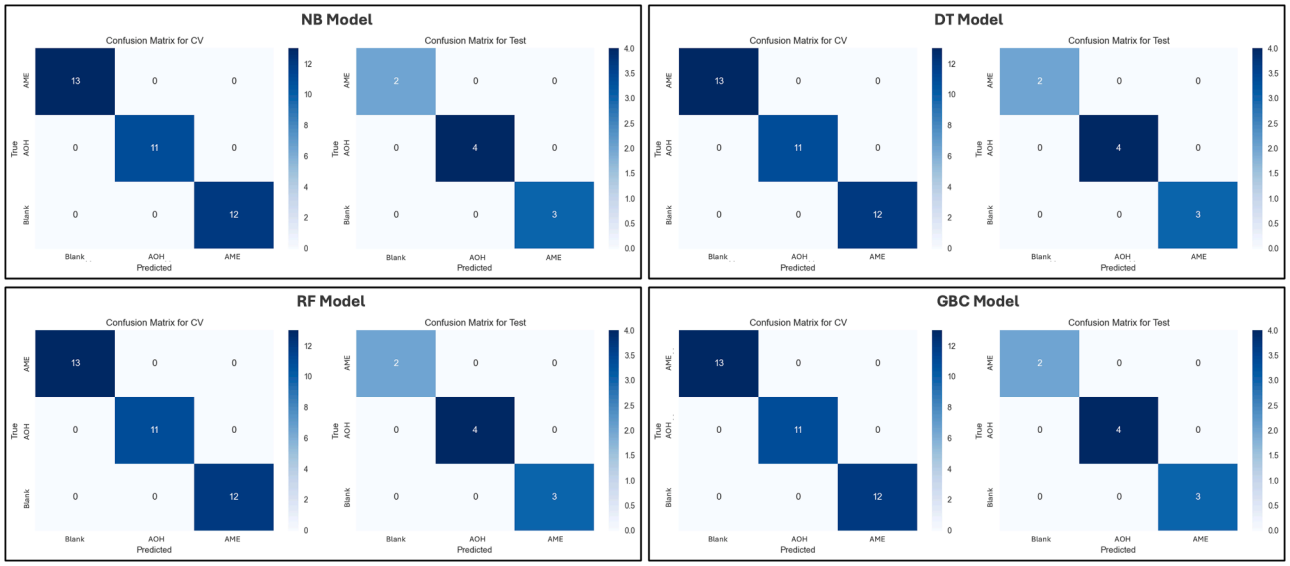


Fig. 4. Confusion matrices for cross-validation (CV) and the test set, obtained by applying the four best-performing algorithms (NB, DT, RF, GBC) to the dataset from DPV (specifically peak currents and potentials).

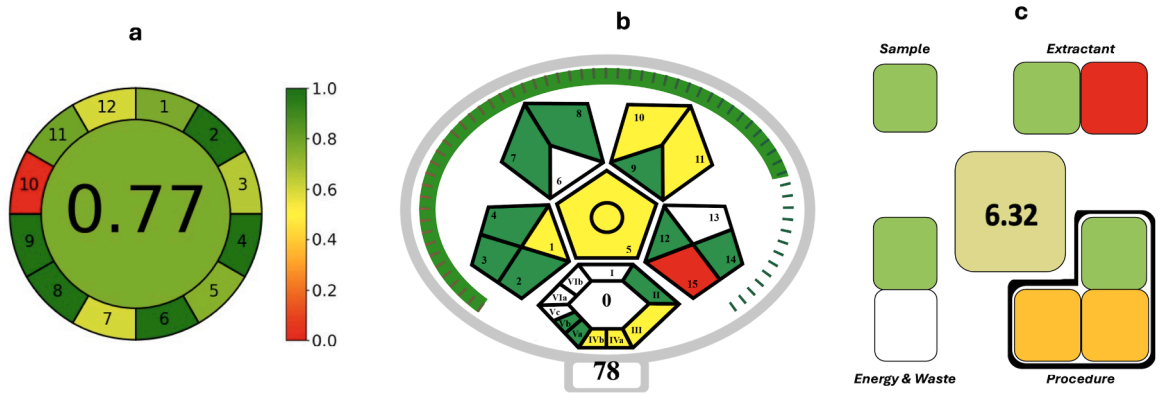


Fig. 5. Analytical greenness scores assessed using the AGREE (a), ComplexMoGAPI (b) and SPMS (c) metric tools for the developed electroanalytical screening platform.

the pentagrams reflects the method's overall performance.

An overall assessment of the greenness of the entire analytical process, including the use of the additional SPMS metric tool, highlights several strengths: highly simplified, rapid and cost-effective sampling and processing of samples; extremely low energy consumption of the reading instrumentation; implementability of Wi-Fi connectivity [49–51] into portable devices for on-line/at-line use in PON settings [52]. The critical aspects related to waste generation since CMEs are single-use and the use of dodecanethiol, a moderately toxic reagent, are offset by the very small quantities required, the extremely low sample volume, and the remarkably short analysis times.

Moreover, the possibility of implementing the ML algorithm needed for data processing on the edge further improves the power consumption of the device and hence the greenness of the approach [53]. Indeed, implementing ML algorithms on the edge offers a greener and more energy-efficient solution, reducing the need for continuous data transmission to centralized cloud servers, which in turn reduces network load and the carbon footprint associated with large-scale data centers. Local data processing also allows for faster response times and greater privacy. However, this approach comes with drawbacks, most notably the limited computational power and storage space available on edge devices, which can limit its applicability to complex models for deployment and update. To balance sustainability and capacity, a hybrid architecture can be adopted, in which lightweight inference runs on the edge, while more computationally demanding tasks—such as model training, optimization, or periodic deep analysis—are offloaded to the cloud. This combination preserves the environmental benefits of edge computing while leveraging the flexibility and scalability of cloud resources when needed. In particular, by balancing transmissions to the centralized server and adopting appropriate power-saving modes available on low-end low-power devices, it is possible to achieve good results consistent with those required by the ComplexMoGAPI tool and presented in Table 3. An example of this approach can be found in [54], where a power consumption of $14e^{-6}$ kWh per sample demonstrates very low energy levels compared to the threshold required by the ComplexMoGAPI tool.

4. Conclusions

This study demonstrates the feasibility of integrating CMEs based on screen-printed gold substrates modified with dodecanethiol SAMs as electroanalytical platforms for the rapid, first-line screening of Alternaria toxins in tomato food products. Optimization of each CME to enhance the electrochemical response to AOH or AME allowed the dual-electrode system, assisted by data-driven algorithms, to effectively discriminate between control tomato samples and those spiked with

Table 3
Scores achieved for the developed electroanalytical screening platform. All AGREE and ComplexMoGAPI metrics criteria were considered.

Greenness metrics			
AGREE		ComplexMoGAPI	
Criterion	Score	Criterion	Score
Sample treatment	0.78	*Sample preparation*	
Sample amount	1.00	Collection	on-line/at-line
Device positioning	0.66	Preservation	none
Sample prep. stages	1.00	Transport	none
Automation, miniaturization	0.75	Storage	none
Derivatization	1.00	Type of method	Simple procedure (filtration /dilution)
Waste	0.60	Scale of extraction	N.A.
Analysis throughput	1.00	Solvent/reagent used	Solvent-free methods
Energy consumption	1.00	Additional treatment	none
Source of reagents	0	Amount	< 10ml (< 10g)
Toxicity	0.80	Health hazard	Moderately toxic; NFPA = 2 or 3
Operator's safety	0.60	Safety hazard	NFPA flammability = 2 or 3
		Instrumentation	
		Energy	≤0.1 kWh per sample
		Occupational hazard	N.A.
		Waste	< 1ml (< 1g)
		Waste treatment	no treatment
		Quantification	yes
		Yield and condition	
		I – Yield	N.A.
		II – Temperature/ time	Room temperature, <1h
		Relation to green economy	
		III – Number of rules met	3-4
		Reagents and solvents	
		IV a – Health hazard	Moderately toxic; NFPA = 2 or 3
		IV b – Safety hazard	
		Instrumentation	
		V a – Technical setup	Common setup
		V b – Energy	≤0.1 kWh per sample
		V c – Occupational hazard	NFPA flammability = 2 or 3
		Workup and purification (N.A.)	

individual toxins. By combining these analytical capabilities with ML algorithms to process the voltammetric dataset for predictive modelling of contamination events and using portable, battery-powered instrumentation, the system becomes an even more powerful first-line screening tool, which can be used for on-site analysis in point-of-need settings, supporting decentralized quality control strategies in the agri-food sector. Indeed, combining the strategy of optimizing the response of two CMEs for each toxin with the implementation of ML-based predictive models significantly improves the ability to detect contamination by at least one of the two toxins, thus limiting the risk of false negatives.

The proposed workflow ensures minimal sample handling, requiring only centrifugation and dilution after the preliminary steps common to all food sample analyses, such as washing, cutting, and homogenization after freezing. It provides analytical results in just minutes.

The assessment of the method's greenness index confirmed its favourable environmental profile. Despite the use of dodecanethiol, a potentially hazardous reagent, the overall impact remains low thanks to the extremely small quantities involved in the electrode modification step. Avoiding organic solvent extraction, using negligible amounts of reagents and minimising waste contribute to a sustainable analytical process that complies with the principles of green analytical chemistry.

Overall, this study establishes a proof of concept for combining surface-engineered electrochemical devices with computational intelligence within a green analytical framework. The results highlight how intelligent, low-cost, and environmentally friendly devices can contribute to safer food chains and advance the transition toward next-generation sustainable analytical technologies feasible for application to real food samples natively contaminated by AOH and/or AME.

Funding source

This work was supported by the METROFOOD-IT project, funded by the European Union-NextGenerationEU, PNRR-Mission 4 "Education and Research" Component 2: from research to business, Investment 3.1: Fund for the realization of an integrated system of research and innovation infrastructures—IR0000033 (D.M. (Ministerial Decree) Prot. n. 120 of 21 June 2022).

CRediT authorship contribution statement

Simone Fortunati: Methodology, Investigation, Formal analysis, Data curation. **Cristian Maffezzoni:** Validation, Methodology, Data curation. **Chiara Giliberti:** Formal analysis, Data curation. **Valentina Bianchi:** Writing – original draft. **Ilaria De Munari:** Writing – review & editing. **Maria Careri:** Writing – review & editing, Writing – original draft, Supervision, Project administration, Methodology, Funding acquisition. **Marco Giannetto:** Writing – review & editing, Writing – original draft, Supervision, Methodology, Conceptualization.

Declaration of competing interest

The authors declare that they have no known competing financial interests or personal relationships that could have appeared to influence the work reported in this paper.

Acknowledgements

This work has benefited from the equipment and framework of the COMP-R Initiative, funded by the 'Departments of Excellence' program of the Italian Ministry for University and Research (MUR, 2023-2027)

Supplementary materials

Supplementary material associated with this article can be found, in the online version, at doi:10.1016/j.greeac.2026.100332.

Data availability

Data will be made available on request.

References

[1] A. Chen, X. Mao, Q. Sun, Z. Wei, J. Li, Y. You, J. Zhao, G. Jiang, Y. Wu, L. Wang, Y. Li, Alternaria mycotoxins: An overview of toxicity, metabolism, and analysis in food, J. Agric. Food Chem. 69 (2021) 7817–7830, https://doi.org/10.1021/acs.jafc.1c03007.
[2] H.B. Lee, A. Patriarca, N. Magan, Alternaria in Food: Ecophysiology, Mycotoxin Production and Toxicology, Mycobiology 43 (2015) 93–106, https://doi.org/10.5941/myco.2015.43.2.93.
[3] G. Pose, A. Patriarca, V. Kyanko, A. Pardo, V.Fernández Pinto, Water activity and temperature effects on mycotoxin production by Alternaria alternata on a synthetic tomato medium, Int. J. Food Microbiol. 142 (2010) 348–353, https://doi.org/10.1016/j.ijfoodmicro.2010.07.017.
[4] EFSA Panel on Contaminants in the Food Chain (CONTAM), Scientific opinion on the risks for animal and public health related to the presence of Alternaria toxins in feed and food, EFSA J. 9 (2011) 2407, https://doi.org/10.2903/j.efsa.2011.2407.
[5] European Food Safety Authority, D. Arcella, M. Eskola, J.A. Gómez Ruiz, Dietary exposure assessment to Alternaria toxins in the European population, EFSA J. 14 (2016) e04654, https://doi.org/10.2903/j.efsa.2016.4654.
[6] R. Khan, F. Anwar, F.M. Ghazali, A comprehensive review of mycotoxins: Toxicology, detection, and effective mitigation approaches, Heliyon 10 (2024) e28361, https://doi.org/10.1016/j.heliyon.2024.e28361. Article.

[7] Commission Recommendation (EU) 2022/553 of, on monitoring the presence of Alternaria toxins in food, OJ L 107 (2022) 90–92, 6.4.2022, https://eur-lex.europa.eu/eli/reco/2022/553/oj/eng.
[8] S.A.S. Bacha, Y. Li, J. Nie, G. Xu, L. Han, S. Farooq, Comprehensive review on patulin and Alternaria toxins in fruit and derived products, Front. Plant Sci. 14 (2023) 1139757, https://doi.org/10.3389/fpls.2023.1139757.
[9] A. Rico-Yuste, J. Walravens, J.L. Urraca, R.A.G. Abou-Hany, A.B. Descalzo, G. Orellana, M. Rychlik, S. De Saeger, M.C. Moreno-Bondi, Analysis of alternariol and alternariol monomethyl ether in foodstuffs by molecularly imprinted solid-phase extraction and ultra-high-performance liquid chromatography tandem mass spectrometry, Food Chem. 243 (2018) 357–364, https://doi.org/10.1016/j.foodchem.2017.09.125.
[10] T. Moya-Cavas, F. Navarro-Villoslada, J.L. Urraca, L.A. Serrano, G. Orellana, M. C. Moreno-Bondi, Simultaneous determination of zearalenone and alternariol mycotoxins in oil samples using mixed molecularly imprinted polymer beads, Food Chem. 412 (2023) 135538, https://doi.org/10.1016/j.foodchem.2023.135538.
[11] L. Xing, L. Zou, R. Luo, Y. Wang, Determination of five Alternaria toxins in wolfberry using modified QuEChERS and ultra-high performance liquid chromatography-tandem mass spectrometry, Food Chem. 311 (2020) 125975, https://doi.org/10.1016/j.foodchem.2019.125975.
[12] J. Zhang, R. Huang, Y. Feng, T. Yang, M. Sun, H. Kuang, C. Xu, L. Guo, Development and validation of stable isotope dilution LC–MS/MS method for simultaneous quantification of four Alternaria toxins in 15 food commodities, Food Chem. 457 (2024) 140122, https://doi.org/10.1016/j.foodchem.2024.140122.
[13] L. Fang, F. Qiu, X. Yu, Y. Wang, Sensitive determination of Alternaria toxins in cereals and cereal-based foods using online MAX SPE column cleanup coupled with liquid chromatography-tandem mass spectrometry, Food Chem. 493 (2025) 145806, https://doi.org/10.1016/j.foodchem.2025.145806. Article.
[14] J. Singh, A. Mehta, Rapid and sensitive detection of mycotoxins by advanced and emerging analytical methods: A review, Food Sci. Nutr. 8 (2020) 2183–2204, https://doi.org/10.1002/fsn3.1474.
[15] J. Wang, T. Peng, X. Zhang, K. Yao, Y. Ke, B. Shao, Z. Wang, J. Shen, H. Jiang, A novel hapten and monoclonal antibody-based indirect competitive ELISA for simultaneous analysis of alternariol and alternariol monomethyl ether in wheat, Food Control 94 (2018) 65–70, https://doi.org/10.1016/j.foodcont.2018.06.027.
[16] S. Hou, Y. Zhang, X. Wang, J. Ma, Y. Cheng, M. Wang, Z. Wang, H. Wang, J. Sun, W. Zhang, Y. xian Yan, Establishment of an immunolateral chromatographic quantitative method for the detection of alternariol based on quantum dot fluorescent nanospheres in fruit, LWT 203 (2024) 116353, https://doi.org/10.1016/j.lwt.2024.116353.
[17] L.G. Addante-Moya, D. Suay-Fuentes, A. Abad-Somovilla, C. Agulló, A. Abad-Fuentes, J.V. Mercader, A rapid monoclonal antibody-based direct immunoassay and a lateral-flow device for on-site sensitive analysis of the mycotoxin alternariol, Microchem. J. 199 (2024) 109892, https://doi.org/10.1016/j.microc.2024.109892. Article.
[18] S. Wang, H. Gao, Z. Wei, J. Zhou, S. Ren, J. He, Y. Luan, X. Lou, Shortened and multivalent aptamers for ultrasensitive and rapid detection of alternariol in wheat using optical waveguide sensors, Biosens. Bioelectron 196 (2022) 113702, https://doi.org/10.1016/j.bios.2021.113702. Article.
[19] M. Jiang, M. Wang, W. Lai, X. Song, J. Li, D. Liu, Z. Wei, C. Hong, Construction of electrochemical and electrochemiluminescent dual-mode aptamer sensors based on ferrocene dual-functional signal probes for the sensitive detection of Alternariol, Anal. Chim. Acta 1272 (2023) 341476, https://doi.org/10.1016/j.aca.2023.341476.
[20] Q. Liu, X. Yang, L. Xiang, X. Li, C. Kang, D. Chen, A fluorescence-assisted SERS aptasensor based on gold nanoflowers for sensitive detection of alternariol, Microchem. J. 219 (2025) 116037, https://doi.org/10.1016/j.microc.2025.116037.
[21] M. Mattarozzi, L. Toma, A. Bertucci, M. Giannetto, M. Careri, Aptamer-based assays: strategies in the use of aptamers conjugated to magnetic micro- and nanobeads as recognition elements in food control, Anal. Bioanal. Chem. 414 (2022) 63–74, https://doi.org/10.1007/s00216-021-03501-6.
[22] L. Toma, M. Mattarozzi, L. Ronda, V. Marassi, A. Zattoni, S. Fortunati, M. Giannetto, M. Careri, Are aptamers really promising as receptors for analytical purposes? Insights into anti-lysozyme DNA aptamers through a multitechnique study, Anal. Chem. 96 (2024) 2719–2726, https://doi.org/10.1021/acs.analchem.3c05883.
[23] M.B. Moressi, A. Zon, H. Fernandez, G. Rivas, V. Solis, Amperometric quantification of Alternaria mycotoxins with a mushroom tyrosinase modified carbon paste electrode, Electrochem. Commun. 1 (1999) 472–476, https://doi.org/10.1016/S1388-2481(99)00096-X.
[24] M. Singh, N. Kaur, E. Comini, The role of self-assembled monolayers in electronic devices, J. Mater. Chem. C 8 (2020) 3938–3955, https://doi.org/10.1039/D0TC00388C.
[25] M.B Moressi, R. Andreu, J.J. Calvente, H. Fernández, M.A. Zón, Improvement of alternariol monomethyl ether detection at gold electrodes modified with a dodecanethiol self-assembled monolayer, J. Electroanal. Chem. 570 (2004) 209–217, https://doi.org/10.1016/j.jelechem.2004.03.031.
[26] M. Giannetto, L. Mori, G. Mori, M. Careri, A. Mangia, New amperometric immunosensor with response enhanced by PAMAM-dendrimers linked via self-assembled monolayers for determination of alpha-fetoprotein in human serum, Sens. Actuators, B Chem. 159 (2011) 185–192, https://doi.org/10.1016/j.snb.2011.06.070.
[27] M. Piergiovanni, C. Giliberti, C. Maffezzoni, D. Errico, M. Blandino, C. Dall'Asta, M. Mattarozzi, F. Bianchi, M. Giannetto, M. Careri, Electronic nose technology for the detection of ergot alkaloid in soft wheat and identification of the relevant volatile compounds by solid phase microextraction/gas chromatography-high resolution Orbitrap-mass spectrometry coupled to chemometrics, Food Chem. 484 (2025) 144455, https://doi.org/10.1016/j.foodchem.2025.144455.
[28] C. Giliberti, G. Magnani, M. Mattarozzi, M. Giannetto, F. Bianchi, M. Careri, S. Cagnoni, Machine learning and evolutionary computation on e-nose datasets: A preliminary approach to ergot alkaloid detection in wheat, Chemometr. Intell. Lab. Syst. 268 (2026) 105574, https://doi.org/10.1016/j.chemolab.2025.105574.
[29] P. Puthongkham, S. Wirojsaengthong, A. Suea-Ngam, Machine learning and chemometrics for electrochemical sensors: moving forward to the future of analytical chemistry, Analyst 146 (2021) 6351–6364, https://doi.org/10.1039/D1AN01148K.
[30] M. Kang, D. Kim, J. Kim, N. Kim, S. Lee, Strategies to enrich electrochemical sensing data with analytical relevance for machine learning applications: A focused review, Sensors 24 (2024) 3855, https://doi.org/10.3390/s24123855.
[31] F. Pena-Pereira, W. Wojnowski, M. Tobiszewski, AGREE—Analytical GREEnness metric approach and software, Anal. Chem. 92 (2020) 10076–10082, https://doi.org/10.1021/acs.analchem.0c01887.
[32] F.R. Mansour, K.M. Omer, J. Płotka-Wasylka, A total scoring system and software for complex modified GAPI (ComplexMoGAPI) application in the assessment of method greenness, Green Anal. Chem., 10 (2024) 100126, https://doi.org/10.1016/j.greeac.2024.100126. Article.
[33] R. González-Martín, A. Gutiérrez-Serpa, V. Pino, M. Sajid, A tool to assess analytical sample preparation procedures: sample preparation metric of sustainability, J. Chromatogr. A 1707 (2023) 464291, https://doi.org/10.1016/j.chroma.2023.464291. Article.
[34] Y. Tang, L. Mu, J. Cheng, Z. Du, Y. Yang, Determination of Multi-Class Mycotoxins in Apples and Tomatoes by Combined Use of QuEChERS Method and Ultra-High-Performance Liquid Chromatography Tandem Mass Spectrometry, Food Anal. Methods 13 (2020) 1381–1390, https://doi.org/10.1007/s12161-020-01753-z.
[35] A.Ch. Lazanas, M.I. Prodromidis, Electrochemical Impedance Spectroscopy-A Tutorial, ACS Meas. Sci. Au. 3 (2023) 162–193, https://doi.org/10.1021/acsmeasuresciau.2c00070.
[36] B. Magnusson, U. Örnemark (Eds.), Eurachem Guide: The Fitness for Purpose of Analytical Methods—A Laboratory Guide to Method Validation and Related Topics, 2nd ed, Eurachem, Gembloux, Belgium, 2014. Available online, http://www.eurachem.org.
[37] R.A. Van den Berg, H.C. Hoefsloot, J.A. Westerhuis, A.K. Smilde, M.J. Van der Werf, Centering, scaling, and transformations: improving the biological information content of metabolomics data, BMC Genom. 7 (2006) 142, https://doi.org/10.1186/1471-2164-7-142.
[38] M. Ali, PyCaret: An open source, low-code machine learning library in Python. PyCaret version, 3.3.2, 2020. https://www.pycaret.org.
[39] F. Pedregosa, G. Varoquaux, A. Gramfort, V. Michel, B. Thirion, O. Grisel, M. Blondel, P. Prettenhofer, R. Weiss, V. Dubourg, J. Vanderplas, A. Passos, D. Cournapeau, M. Brucher, M.P.É. Duchesnay, Scikit-learn: Machine learning in Python, J. Mach. Learn. Res. 12 (2011) 2825–2830, 2011, https://www.jmlr.org/papers/volume12/pedregosa11a/pedregosa11a.pdf?source=post_page.
[40] A.J. Smola, B. Schölkopf, A tutorial on support vector regression, Stat. Comput. 14 (2004) 199–222, https://doi.org/10.1023/B:STCO.0000035301.49549.88.
[41] T.K. Ho, The random subspace method for constructing decision forests, IEEE Trans. Pattern Anal. Mach. Intell. 20 (1998) 832–844, https://doi.org/10.1109/34.709601.
[42] P.P. Goswami, A.V. Singh, S.G. Singh, ZnO nanoflower-mediated paper-based electrochemical biosensor for perfect classification of cardiac biomarkers with physics-informed machine learning, Mikrochim. Acta 192 (2025) 1–13, https://doi.org/10.1007/s00604-025-07102-3.
[43] D.J. Hand, K. Yu, Idiot's Bayes—not so stupid after all? Int, Stat. Rev. 69 (2001) 385–398, https://doi.org/10.2307/1403452.
[44] B.A. Tama, S. Lim, Ensemble learning for intrusion detection systems: A systematic mapping study and cross-benchmark evaluation, Comput. Sci. Rev. 39 (2021) 100357, https://doi.org/10.1016/j.cosrev.2020.100357.
[45] O. Hammerich, B. Speiser (Eds.), Organic electrochemistry, CRC press, Boca Raton, 2016, https://doi.org/10.1201/b19122.
[46] E. Sabatani, I. Rubinstein, Organized self-assembling monolayers on electrodes. 2. Monolayer-based ultramicroelectrodes for the study of very rapid electrode kinetics, J. Phys. Chem. 91 (1987) 6663–6669, https://doi.org/10.1021/j100311a021.
[47] M. Piergiovanni, V. Termopoli, C. Maffezzoni, N. Riboni, V. Consonni, F. Bianchi, M. Mattarozzi, D. Ballabio, M, Careri Condensed phase membrane introduction mass spectrometry: A new frontier for the real-time monitoring of hazardous chemical migration from food contact materials, Green Anal. Chem. 12 (2025) 100199, https://doi.org/10.1016/j.greeac.2024.100199. Article.
[48] A. Ganesan, K.P. Kannaiah, H.K. Chanduluru, A comprehensive review of green, white analytical chemistry metrics and their application across the liquid chromatographic method lifecycle (2024–2025), Microchem. J. 219 (2025) 116187, https://doi.org/10.1016/j.microc.2025.116187. Article.
[49] V. Bianchi, A. Boni, S. Fortunati, M. Giannetto, M. Careri, I. De Munari, A Wi-Fi Cloud-Based Portable Potentiostat for Electrochemical Biosensors, IEEE Trans. Instrum. Meas. 69 (2020) 3232–3240, https://doi.org/10.1109/TIM.2019.2928533.
[50] V. Bianchi, A. Boni, M. Bassoli, M. Giannetto, S. Fortunati, M. Careri, I. De Munari, IoT and biosensors: a smart portable potentiostat with advanced cloud-enabled features, IEEE Access 9 (2021) 141544–141554, https://doi.org/10.1109/ACCESS.2021.3120022.
[51] G. Magnani, C. Giliberti, D. Errico, M. Stighezza, S. Fortunati, M. Mattarozzi, A. Boni, V. Bianchi, M. Giannetto, I. De Munari, S. Cagnoni, M. Careri, Evaluation

of a Voltametric E-tongue combined with data preprocessing for fast and effective machine learning-based classification of tomato purées by cultivar, Sensors 24 (2024) 3586, https://doi.org/10.3390/s24113586.

[52] C. Giliberti, M. Malavasi, S. Fortunati, L. Cattani, M. Giannetto, S. Rainieri, M. Careri, On-Line Monitoring of Vitamin C in Fruit Juice in Processing Plants by Electrochemical Sensor Based on PEDOT-Modified Electrodes: A Feasibility Study, Sensors 25 (2025) 1385, https://doi.org/10.3390/s25051385.

[53] M. Stighezza, G. Magnani, V. Bianchi, S. Cagnoni, A. Boni, C. Giliberti, D. Errico, S. Fortunati, M. Giannetto, M. Careri, I. De Munari. Model-Based design of a Machine Learning algorithm for on-site food authenticity testing, MetroInd4.0 & IoT, 2024, pp. 43–47, https://doi.org/10.1109/MetroInd4.0IoT61288.2024.10584131.

[54] M. Stighezza, I. De Munari, M. Caselli, A. Boni, V. Bianchi, A Flexible Multichannel Platform for Versatile E-Nose and E-Tongue Operations, IEEE Trans. Instrum. Meas. 74 (2025) 2006214.